JOURNAL OF PROPULSION AND POWER
Vol. 10, No. 4, July–Aug. 1994

Use of Permanent Magnets to Reduce Anode Losses in MPD Thrusters

A. D. Gallimore,* A. J. Kelly,† and R. G. Jahn‡
Princeton University, Princeton, New Jersey 08544

Results from previous studies indicate that the anode fall, the principal source of anode heating in MPD thrusters, increases monotonically with the electron Hall parameter calculated from electron temperature, number density, and magnetic field data obtained near the anode. In an attempt to reduce the anode fall by decreasing the local electron Hall parameter, a proof-of-concept test was performed in which an array of 36 permanent magnets were embedded within the anode of a high-power quasisteady MPD thruster to decrease the local azimuthal component of the induced magnetic field. The modified thruster was operated at power levels between 150 kW and 4 MW with argon and helium propellants. Terminal voltage, triple probe, floating probe, and magnetic probe measurements were made to characterize the performance of the thruster with the new anode. Incorporation of the modified anode resulted in a reduction of the anode fall by up to 15 V with argon and 20 V with helium, which corresponded to decreased anode power fractions of 40 and 45% with argon and helium, respectively.

Nomenclature

B = magnetic field strength, T
e = elementary charge, 1.6×10^{-19} C
j_a = anode current density, A/cm^2
k = Boltzmann's constant, 1.38×10^{-23} J/K
m_e = electron mass, 9.11×10^{-31} kg
n_e = electron number density, m^{-3}
$\dot{q}_a$ = anode heat flux, W/cm^2
$\dot{q}_c$ = anode heat flux from convection, W/cm^2
$\dot{q}_r$ = anode heat flux from radiation, W/cm^2
T_e = electron temperature, K
V_a = anode fall, V
Z = axial direction
ε_0 = permittivity of free space, 8.85×10^{-12} F/m
Θ = azimuthal angle
Λ = plasma parameter
λ_e = electron Debye length, m
ϕ = anode material work function, 4.62 V
Ω_e = electron Hall parameter

Introduction

IT has long been established that a propulsion system of high exhaust velocity is desirable for interplanetary space missions. A review of the rocket equation shows that in order for a propulsive system not to require an inordinate amount of propellant for a given space mission, its exhaust velocity should be at least of the same order as the characteristic velocity increment required for the mission. For most interplanetary missions, a characteristic velocity increment of at least 10 km/s is necessary.[1–4] Because of its potential for achieving extremely large exhaust velocities (>40 km/s), the MPD thruster is well suited for these ambitious space missions. The utility of the device in this role, however, is severely hampered by its low thrust efficiency[5–7] as a result of frozen-flow and anode losses. At the thruster power levels proposed for various space missions (i.e., <2 MW), a large fraction of the input power of the engine is wasted in heating the anode.[8,9] Furthermore, given the fact that the anode heat flux of such a device can easily exceed 1 kW/cm^2,[8,9] the prospect of designing anodes with adequate lifetimes (thousands of hours) is, at this point, uncertain at best. Therefore, methods must be developed to reduce the amount of thruster power that is deposited into the anode of MPD thrusters if these devices are to be used for spacecraft propulsion.

Background

The local anode heat flux to a small region of the anode where plasma properties do not change appreciably can be written as[10]

$$\dot{q}_a = j_a[V_a + \tfrac{5}{2}(kT_e/e) + \phi] + \dot{q}_c + \dot{q}_r \qquad (1)$$

wherein all quantities are averaged over the portion of the anode of interest. In this equation, the anode heating sources are represented by voltages multiplied by the anode current density. The anode fall, which is the voltage associated with the region of intense electric fields near the anode, can exceed 40 V in high-powered MPD thrusters.[8,9] In comparison, the voltages associated with energy the anode absorbs from the random thermal energy of the current carrying electrons and due to the work function of the anode material are each usually between 3–10 V. The heat flux to the anode due to convection and radiation has been estimated to be negligible for high-powered thrusters.[8,11–13] Therefore, under most operating conditions, the kinetic energy that electrons gain from the anode fall and deliver to the anode is the dominant mechanism of delivering energy to the anode of high-powered MPD thrusters.

Studies have shown that the anode fall increases monotonically with the local electron Hall parameter.[9,14] The electron Hall parameter is a measure of the response of electrons to electric and magnetic fields. In plasmas with low electron Hall parameters, current carrying electrons flow parallel with the electric field while in plasmas with large electron Hall parameters, electrons tend to migrate in a direction that is perpendicular to both the electric and magnetic fields. For a fully

Presented as Paper 92-3461 at the AIAA/SAE/ASME/ASEE 28th Joint Propulsion Conference and Exhibit, Nashville, TN, July 6–8, 1992; received July 24, 1992; revision received Jan. 6, 1994; accepted for publication Jan. 10, 1994.

*Graduate Student, Department of Mechanical and Aerospace Engineering, Electric Propulsion Laboratory; currently Assistant Professor, Department of Aerospace Engineering, University of Michigan, Ann Arbor, Michigan 48109. Member AIAA.

†Manager and Senior Research Engineer, Electric Propulsion Laboratory. Member AIAA.

‡Professor, Department of Mechanical and Aerospace Engineering, Electric Propulsion Laboratory. Fellow AIAA.

ionized plasma, the electron Hall parameter is evaluated by the following:

$$\Omega_e = \frac{3(2\pi)^{3/2}\varepsilon_0^2}{\sqrt{m_e}\ /\!/\ \Lambda}\frac{(kT_e)^{3/2}B}{e^3 n_e} \tag{2}$$

where the plasma parameter is given by

$$\Lambda = 9(\tfrac{4}{3})\pi n_e \lambda_e^3 \tag{3}$$

and where the electron Debye length is calculated from the following equation:

$$\lambda_e = \sqrt{\varepsilon_0 kT_e/n_e e^2} \tag{4}$$

Ignoring the weak dependence of $/\!/\ \Lambda$ on n_e, Eq. (2) shows that the electron Hall parameter is proportional to electron temperature raised to the 3/2th power and the magnetic field strength, and is inversely proportional to electron number density. Therefore, two approaches to reducing anode power dissipation may be to decrease the electron Hall parameter either by increasing the electron number density through anode propellant injection or decreasing the local magnetic field strength through the use of a counteracting applied magnetic field.

The difficulty in using propellant injection to reduce the Hall parameter is that in order for this injected mass to significantly increase the local electron collision frequency without degrading thruster performance, a substantial fraction of it needs to be ionized over a length scale commensurate with the anode fall region. Careful matching of the anode injection flow rate with thruster operating conditions is necessary to insure that this injected mass does not simply decrease the thruster specific impulse without significantly reducing anode power deposition. Attempts at decreasing the anode heating rate via the injection of propellant through or near the anode have produced inconclusive results.[15-17] In most cases, the anode fall is only slightly reduced with little or no effect on efficiency. Since these studies were performed on thrusters operating at low exhaust velocities (<20 km/s) in which electrothermal thrust contributions are significant, no conclusive verdict on the utility of anode propellant injection for MPD thrusters operating with electromagnetically accelerated plasmas is yet on hand.

In principle, the other approach to reducing the Hall parameter can be achieved if permanent magnets (or electromagnets) are arranged in the anode in such a manner that the applied field counteracts the local azimuthal field induced by the current. Thus, an anode with permanent magnets embedded within should operate with a lower anode fall and a reduced anode heating rate. As an initial attempt of testing this concept, 36 permanent magnets were embedded within the anode of a high-power quasisteady MPD thruster. The results of this proof-of-concept experiment were promising.

Experimental Apparatus

All experiments are performed in a Plexiglas® vacuum tank that is 1.83 m long with an i.d. of 0.92 m. Tank pressure is maintained at less than 0.02 Pa (1×10^{-4} T) prior to thruster operation by a 15-cm oil diffusion pump backed by two mechanical pumps. The tank contains an electronically controlled probe positioning table with three DOF as well as angular freedom in the horizontal plane. Thruster power is supplied by a 160-kJ pulse-forming network (capacitor bank) capable of delivering a rectangular current pulse of up to 52 kA for a duration of approximately 1 ms (cf. Fig. 1).

The MPD thruster used for this experiment consists of an aluminum cylindrical thrust chamber 5 cm deep with an i.d. of 15.0 cm, and an o.d. of 18.8 cm. The inner surface of the thrust chamber is insulated from the discharge by a Pyrex® tube with a wall thickness of ~1 cm. The cathode, which is

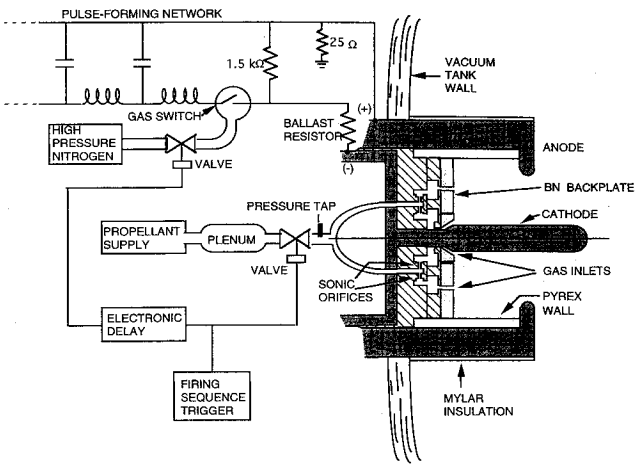

Fig. 1 Quasisteady MPD thruster apparatus.

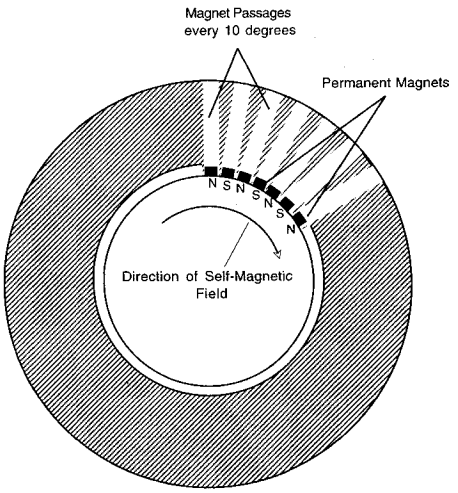

Fig. 2 Front view of MAHP anode.

10 cm long and 1.8 cm in diam, is made of 2% thoriated tungsten. The upstream end of the thrust chamber is enclosed by a boron-nitride backplate. Propellant is injected through the backplate via 12 3-mm-diam holes at a radius of 3.8 cm, and through an annulus at the base of the cathode. An equal amount of propellant flows through the holes and the annulus.

The modified anode used in this study — the Magnetically Annulled Hall Parameter (MAHP) anode — is machined from a 1-cm-thick aluminum ring of o.d. 19 cm, and with an i.d. of 10 cm. All but the lip of the anode is insulated from the discharge with a thick nylon cover. The uninsulated surface area of the MAHP anode is identical to that of the modified benchmark thruster anode studied in Ref. 9.

To minimize the azimuthal magnetic field, the cancellation magnetic field strength should be of the order of that induced by the discharge current. Prior measurements[9] show that the desired range of the field cancellation strength from the permanent magnets at the midlip of the anode should be between 120–1000 G. On the basis of their small size and intense magnetic field (3000 G), cylindrical neodinium-iron-boron magnets, nominally 0.64 cm in diam and 0.32 cm high with poles (N-S) on either face, were selected to produce the cancellation field.

To generate an azimuthal cancellation field, the magnets are placed at the bottom of 36 cylindrical passages machined in the anode (cf. Fig. 2). These passages, each 0.68 cm wide and 4.02 cm deep with a flat base, are placed in 10-deg increments in the azimuthal direction. The top of the passages are threaded (5/16" 24) for a length of approximately 1.3 cm, and each magnet passage comes to within 0.32 cm of the midlip surface and 0.140 cm of the downstream anode face.

The magnets are attached to the unthreaded ends of brass placement rods, which are then inserted into the 36 passages. The magnets are arranged in an alternating pattern (N-S-N, . . . , etc.) with half of the magnets' north pole facing toward the cathode (just beneath the anode surface) and half of the magnets' south pole facing toward the cathode. The magnetic field strength and distribution of the entire array is adjusted by changing the depth of each element.

To determine a satisfactory configuration of the permanent magnets (i.e., depth of each element) which ensures that a uniform cancellation field of adequate strength is generated, the MAHP anode was clamped to the rotating table of a milling machine where a Hall probe, anchored to a hinged boom that was attached to the milling machine collar, was used to make precise magnetic field maps near the anode surface. This Hall probe assembly allowed for magnetic field measurements to be made with a spatial resolution of 0.25 mm at an accuracy of 1%.

Figure 3 shows the static (zero thruster current) azimuthal magnetic field strength as a function of azimuthal angle. A least-squares curve fit is also presented to show the sinusoidal variation of the azimuthal field strength with angle. These measurements, made with the Hall probe assembly described above, were taken 1 mm from the anode surface (midlip) where the peak magnetic field strength is approximately 250 G. As the figure clearly illustrates, the alternating polarity of the magnets produces regions along the anode where the local azimuthal field generated by the current is either canceled or reinforced. Therefore, current continuity is expected to be maintained primarily within bands along the anode where the local magnetic field is minimum (field cancellation zones). End-on photographs of the MAHP thruster in operation which show luminous bands within the cancellation zones qualitatively support this prediction.[11]

Figure 4 shows the static azimuthal field strength measured 1 mm from the anode midlip as a function of azimuthal angle and axial position. The line of peak values ($Z = 0$) corresponds to data measured at the anode midplane (cf. Fig. 3). As the figure shows, the strength of the azimuthal magnetic field diminishes rapidly in either direction away from the midplane. The magnetic field profile is also symmetric in the axial and azimuthal directions.

In addition to an azimuthal magnetic field component, the permanent magnets generate radial and axial field components as well. The interaction of these magnetic field components with axial, radial, and azimuthal currents could adversely affect thruster performance. This problem might be avoided if the MAHP anode's magnetic field is significant in comparison to the induced field only within a narrow region near the anode that encompasses the anode fall (~3 mm from the anode surface). To measure the extent of this region, the radial variation of the static azimuthal magnetic field strength as a function of azimuthal angle was measured with the Hall probe assembly described above.

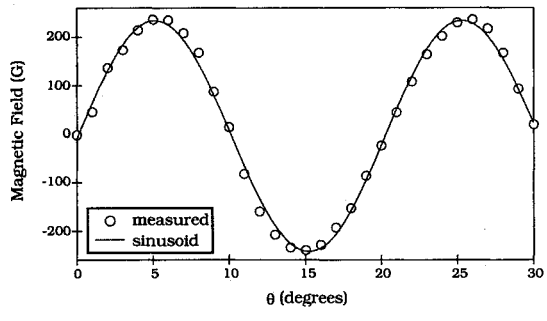

Fig. 3 Anode surface static field profile 1 mm from anode surface (θ—azimuthal direction, Z—axial direction).

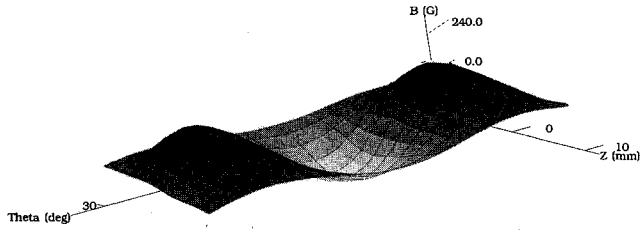

Fig. 4 Static azimuthal magnetic field vs axial position and azimuthal angle (1 mm radially inward from anode midlip radius).

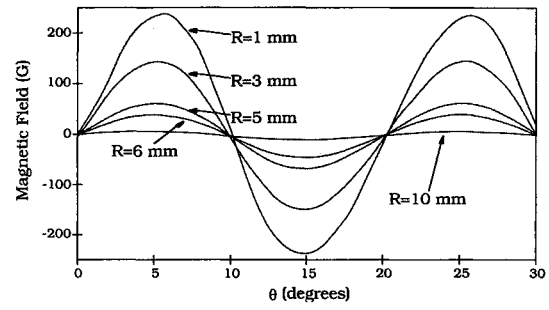

Fig. 5 Static magnetic field radial profile (along midlip).

Figure 5 shows the static azimuthal magnetic field strength as a function of azimuthal angle measured at various radial distances from the anode surface. The peak azimuthal magnetic field strength decreases by a factor of 2 over a span of 2 mm, and by a factor of 5 over 4 mm. A negligible azimuthal magnetic field is measured 1 cm from the anode. As is evident from the figures, the magnetic field of the permanent magnets should have little effect on plasma more than 5 mm from the anode and no effect on plasma 1 or more cm from the anode lip. This implies that because of the small volume in which the magnetic field of the permanent magnets is felt by the plasma, the thrust performance of the thruster is not expected to be significantly affected by the permanent magnets. This statement is tempered somewhat by the fact that electric potential surveys made near the anode (presented below) suggest that the influence of the MAHP anode is felt by plasma 1 cm from the anode surface.

Diagnostics

The primary goals of the experiment were 1) to verify that reduction of the local Hall parameter by use of magnetic field cancellation leads to a decrease in the anode fall; and 2) to map the general operating characteristics of the MAHP thruster, to permit comparison with standard or modified benchmark thruster behavior.

In support of these goals, a number of diagnostic tools have been implemented. A floating langmuir probe is used to make plasma potential measurements from 0.1 to 1.0 cm from the anode surface. The probe is shaped in the form of an "L" to allow for probing near the anode upstream of the midlip. The probe has a 54-cm-long, 0.8-cm-diam arm that is made of G-10 (fiberglass-epoxy composite), and a 1.4-cm-long, 0.25-cm-diam alumina arm that is perpendicular to the G-10 arm. The sensing element of the probe is a tungsten wire electrode 0.026 cm (10 mils) in diam and 0.17 cm (65 mils) long. A small brass clamp is used to connect the tungsten probe electrode to the core of a RG 174 coaxial cable that runs through a 48-cm-long brass tube (o.d. 5 mm) enclosed in G-10 arm. Tygon tubing feeds the coaxial cables from the G-10 tube to the exterior of the tank via a port, thus preventing the cables from outgassing inside of the tank.

Probe and anode potentials are measured with calibrated Nicolet M12 10:1 and Nicolet M12 1:1 voltage probes. Voltage probe outputs are measured with a Tektronix AM501 operational amplifier with matched impedance (10^8 Ω) connected to a Nicolet 320 digital oscilloscope. Oscilloscope traces are transferred to an AT&T personal computer for processing. Curve fits of Laframboise's exact solution of current collection by a cylindrical probe are used to reduce floating probe data

(for the special case of zero probe current collection).[18-21] Floating probe measurements are accurate to within ±2 V.

A triple langmuir probe is employed to measure electron temperatures that are needed both to convert floating potentials to actual plasma potentials and for the estimate of the anode heat flux from measured anode falls [Eq. (1)]. A description of the triple probe system and data reduction algorithm used for this experiment is presented in Ref. 8. Probe construction is similar to that of the floating probe described above. Through the use of Laframboise's analysis, electron temperature and ion number density measurements are accurate to within 10 and 60%, respectively.[20]

A magnetic induction probe is used to measure the ambient magnetic field during thruster operation. The core of this probe consists of a coil with 30 turns of no. 44 Formvar®-coated copper wire on a 0.15-cm-diam Lucite® rod. The core and probe signal lines are enclosed in a quartz tube that is 61 cm long with an o.d. of 4 mm. One end of the quartz tube terminates to form a hemisphere which protects the core from the discharge. The total uncertainty in magnetic field measurements is estimated to be 2%.[22] Further details of the construction, calibration, and operation of the probe can be found in Ref. 22.

Experimental Results

Figure 6 shows the voltage-current characteristics of the benchmark thruster used in Ref. 9 ("standard") and the MAHP thruster ("magnet"). When helium is used as the propellant, the terminal voltage of the MAHP thruster is within 5% of the corresponding value for the benchmark thruster. Thus, no significant change in the voltage-current characteristic is observed when the MAHP anode is operated with helium. However, when operating with argon at a mass flow rate of 16 g/s, over the entire range of current investigated the terminal voltage of the MAHP thruster is consistently a few volts less than corresponding voltage of the benchmark thruster. At 4 g/s (argon), the terminal voltage of the MAHP thruster is as much as 20% (15 V) lower than that of the benchmark thruster at discharge currents between 11–17 kA.

The magnetic field at locations of self-field cancellation and addition are shown in Fig. 7. These data were collected with the magnetic field probe (B-probe) positioned 3 mm from the anode midlip at adjacent field cancellation and enhancement zones. The presence of the field generated by the magnets are clearly shown in this figure. At all thruster operating

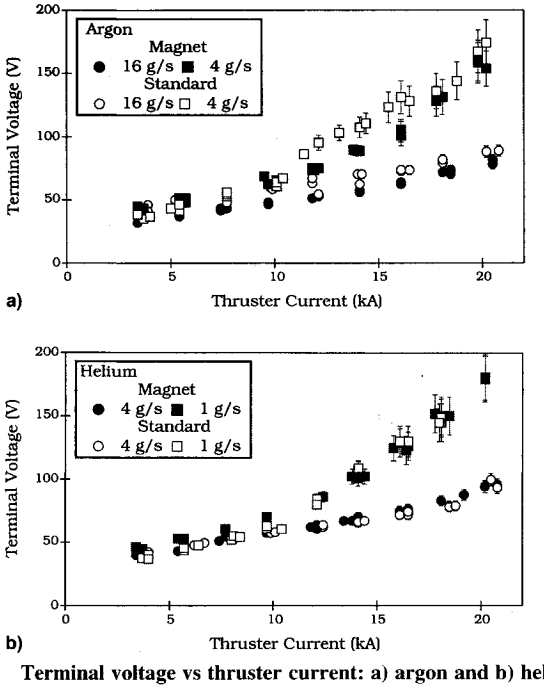

Fig. 6 Terminal voltage vs thruster current: a) argon and b) helium.

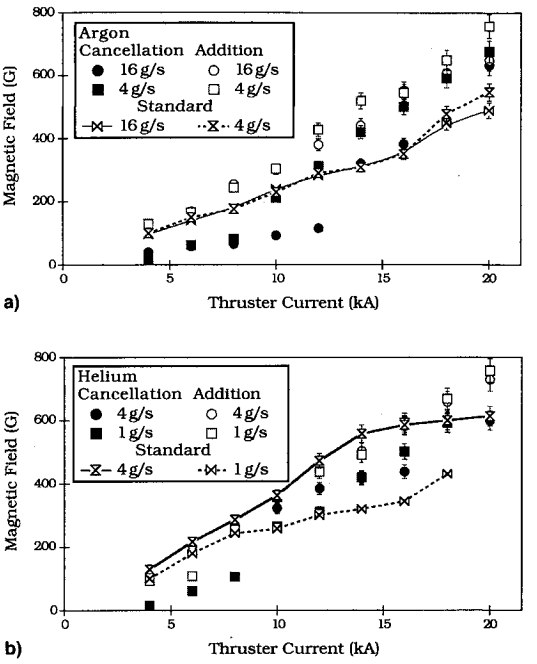

Fig. 7 Magnetic field vs thruster current: a) argon and b) helium.

conditions, the measured field strengths in the cancellation zones are less than those in regions of field addition. An abrupt increase in the magnetic field strength in the cancellation zone is seen at currents of 10 and 14 kA for argon mass flow rates of 4 and 16 g/s, respectively. Moreover, after this transition has taken place, the magnetic field strengths of cancellation regions tend to be higher than the corresponding field strengths measured near the standard benchmark thruster anode.

Similar behavior is exhibited with helium data. At currents below 10 kA, the cancellation zone magnetic field strengths, which are almost identical for either helium propellant flow rate, are significantly lower than those of the standard benchmark thruster and those measured within adjacent zones of field addition. Above 10 kA and at a helium flow rate of 1 g/s, the cancellation and enhancement zone field strengths are higher than the corresponding benchmark thruster field strengths measured at the anode midlip. When operating with helium at a flow rate of 4 g/s and discharge currents between 10–18 kA, the magnetic field strengths in either zone of the MAHP thruster are less than corresponding values of the standard benchmark thruster. However, beyond this current, magnetic field strengths measured in either zone are larger than those corresponding to the benchmark thruster.

The abrupt jumps in magnetic field strength within the cancellation zone occur when the magnitude of induced azimuthal magnetic field approaches that produced by the MAHP anode (~200 G). This implies that a significant redistribution of current along the anode takes place at these transition conditions. A similar phenomenon occurs at low discharge currents where the magnitude of the induced magnetic field near the anode is less than that produced by the permanent magnets. In this case, regions along the anode may exist in which the azimuthal component of the overall magnetic field is in the retrograde direction of the induced field. This configuration is unstable and results in an abrupt shift of the current distribution.

Figures 8 and 9 show electron temperatures and ion number densities measured 2 mm from the anode midlip via triple probe for the MAHP and benchmark thruster. The electron temperatures and ion number densities near the anode of either thruster for either propellant range from 0.8 to 4 eV, and 5×10^{18} to 4×10^{20} m^{-3}, respectively. Temperatures and number densities for the modified anode are virtually identical in either zone. For operation at the highest

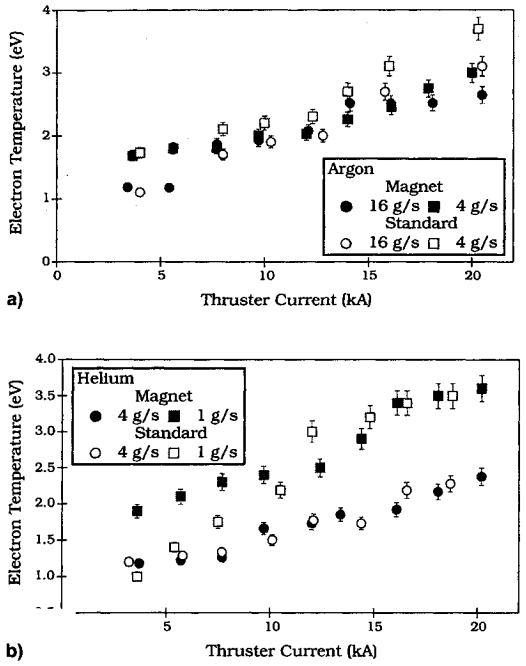

Fig. 8 Electron temperature vs thruster current: a) argon and b) helium.

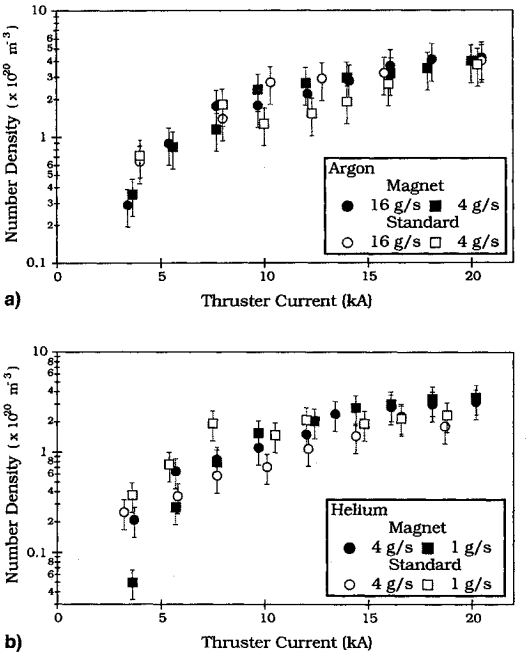

Fig. 9 Ion number density vs thruster current: a) argon and b) helium.

mass flow rate of either propellant, the attenuation of the local magnetic field does not significantly affect the electron temperature. However, at currents below 10 kA with a helium mass flow rate of 1 g/s, the electron temperature for the MAHP anode is almost twice as high as that of the benchmark thruster. The reason for this behavior is unknown. With the thruster operating on argon at 4 g/s, at currents above 12 kA the electron temperatures of the MAHP thruster are between 7 and 25% lower than corresponding values measured in the benchmark thruster.

A source of concern was the possibility that ablated insulator material might be ionized by the discharge and affect current transport to the anode by artificially increasing the number of local current carriers. However, with the exception of the helium data at 4 kA-1 g/s, the number densities near the anode for either engine are virtually the same. Therefore,

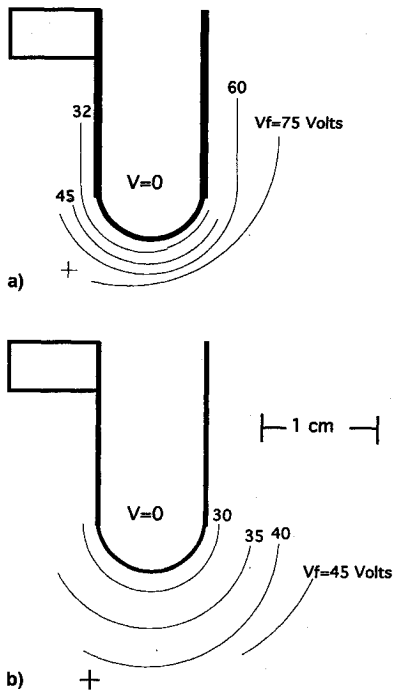

Fig. 10 Anode floating potential profiles (16 kA-4 g/s: argon): a) modified benchmark thruster and b) MAHP thruster.

the amount of charged particles introduced to the discharge near the anode by ionization of ablated insulator material does not appear to be significant.

Figure 10 shows equipotential contours measured near the anode of the modified benchmark thruster and MAHP thruster at a current of 16 kA and an argon propellant flow rate of 4 g/s. The cross in the figure is indicative of the positioning error of the probe rack (± 1 mm). The maximum floating potential measured 1 cm from the MAHP anode is 45 V; considerably less than the 75 V measured the same distance away from the modified benchmark thruster anode. However, the floating potential measured 1 mm from the anode surface of either thruster is approximately 30 V.

Several azimuthal sites, both in cancellation and addition zones of the MAHP anode, were surveyed. Only a minor variation (5%) in floating potential gradient is observed from zone to zone. For all operating conditions, the gradients of floating potential near the MAHP anode are considerably smaller than those of the benchmark thruster anode. Furthermore, the influence of the permanent magnets on the plasma extends beyond the region at which the static magnetic field of the MAHP anode is significant (cf. Fig. 5). This suggests that the magnetic field generated by the MAHP anode is convected into the flowing plasma over a considerably larger volume of the thrust chamber than is suggested by the static field survey.

Electron temperatures obtained with the triple probe are used in converting probe floating potentials to plasma potentials. Figure 11 shows plasma potentials measured 1 mm from the anode surface (herein defined as the anode fall) in cancellation zones as a function of thruster current. The anode fall varies by less than ± 3 V along the lip and ± 5 V between zones (cancellation and enhancement). When the thruster is operating with argon at currents below 12 kA, the anode falls for the modified device are higher than those of the benchmark thruster. However, the anode fall of the MAHP thruster is significantly less than that of the benchmark thruster at currents above 15 kA for an argon flow rate of 16 g/s, and 18 kA for an argon flow rate of 4 g/s. With argon propellant, the MAHP anode reduces the anode fall by as much as 15 V (37%).

When using helium at a propellant mass flow rate at 4 g/s, the anode falls of the modified device are less than those of

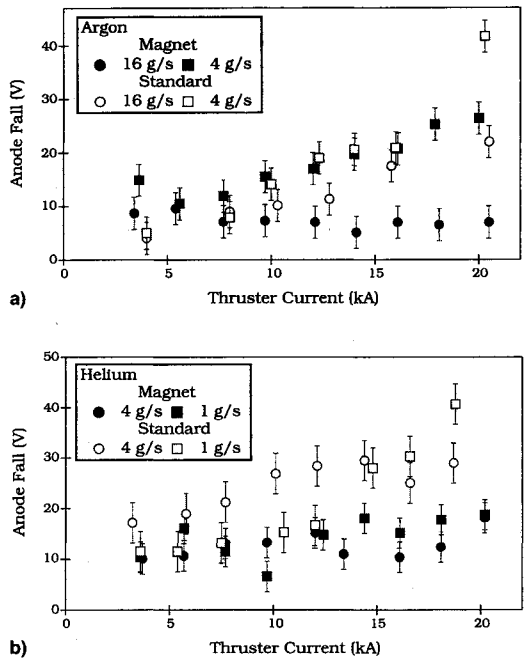

Fig. 11 Anode fall vs thruster current: a) argon and b) helium.

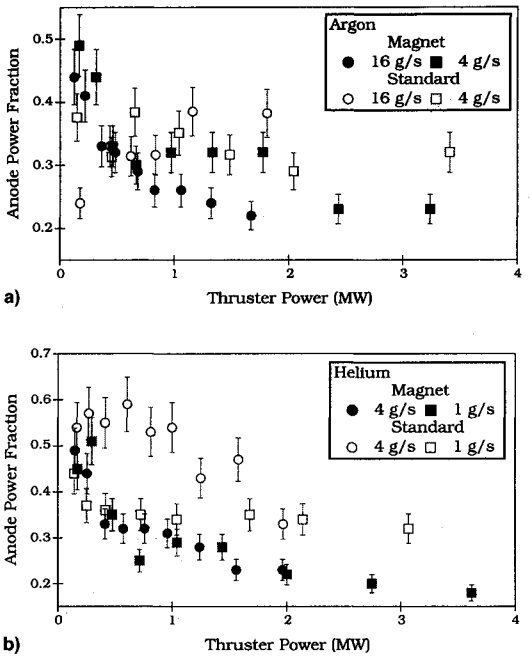

Fig. 12 Anode power fraction vs thruster power: a) argon and b) helium.

the standard thruster throughout the entire range of operation, again irrespective of zone type. At 1 g/s, the anode falls of the MAHP thruster are significantly lower than those of the standard thruster at currents above 12 kA. Incorporation of the MAHP anode results in a reduction of the anode fall by up to 20 V (50%) with helium.

The primary function of the MAHP anode is to reduce the anode power fraction. In Fig. 12, anode power fractions calculated by integrating Eq. (1) over the entire anode surface (assuming azimuthal symmetry) are plotted as a function of thruster power for the MAHP and benchmark thrusters. With argon as propellant and at power levels less than 0.5 MW, the MAHP anode power fractions are higher than those of the original device, varying between 0.3–0.5. At 4 g/s, the anode power fractions of both thrusters are equal within a power range of 0.5–2 MW. Beyond 2 MW, however, the anode power fraction of the MAHP thruster falls to 0.23, a

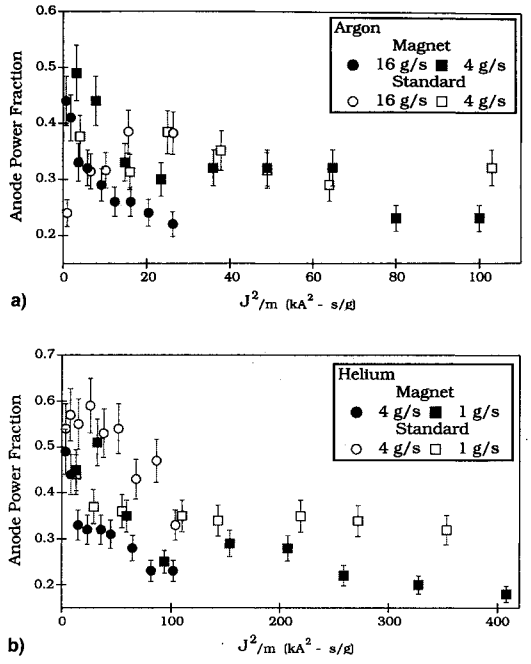

Fig. 13 Anode power fraction vs $J^2/\dot{m}$: a) argon and b) helium.

25% improvement over the standard benchmark thruster. When using argon at 16 g/s, the MAHP thruster operates at lower anode power fractions for power levels above 0.8 MW. With an argon flow rate of 16 g/s and a discharge current of 20 kA, the MAHP anode reduces the anode power fraction by over 40% (0.38–0.22).

During operation with helium at 1 g/s for thruster power levels below 0.4 MW, the anode power fractions of the MAHP thruster are higher than those of the standard benchmark device by as much as 27% (0.51–0.37). At higher power levels, however, the MAHP anode provides sizable reductions of the anode power fraction (e.g., 37% at 3 MW). For operation with helium at 4 g/s, the MAHP anode results in reduced anode power fractions over the entire range of operation. At 18 kA-4 g/s (helium) e.g., the MAHP anode reduces the anode power fraction by 45%, the most significant decrease of the anode power fraction observed in the study.

Anode power fractions for both the MAHP and the modified benchmark thruster are shown as a function of $J^2/\dot{m}$ in Fig. 13. Using the Maecker thrust equation, which has been shown to be accurate for self-field MPD thruster operation in a regime in which most of its thrust is derived from electromagnetic forces ($J^2/\dot{m}$ above 55 and 135 kA^2-s/g for argon and helium propellants, respectively),[23,24] the maximum specific impulse achieved in this study is estimated to have been 1600 s (16 km/s) for argon and 6400 s (64 km/s) with helium. The trends exhibited with thruster power (cf. Fig. 12) are evident with $J^2/\dot{m}$ as well.

Figure 14 shows the anode fall as a function of Hall parameter calculated from Eq. (2) using triple probe and cancellation zone magnetic probe data described above. As the figure illustrates, the correlation between the anode fall and the Hall parameter (cf. Fig. 14) appears in the MAHP anode data as well. Given the large error associated with these calculations (due primarily to uncertainty in number density estimates), it is difficult to determine to what extent the MAHP anode reduces the Hall parameter at the point of current attachment.

Figure 14b shows that the anode falls of the MAHP anode are lower than those of the benchmark anode even at conditions of large local Hall parameter, implying that the MAHP anode may have reduced the sensitivity of the anode fall on the Hall parameter perhaps by bending the magnetic field lines so that they intersect the anode. This trend is observed for operating conditions at which the current is blown down-

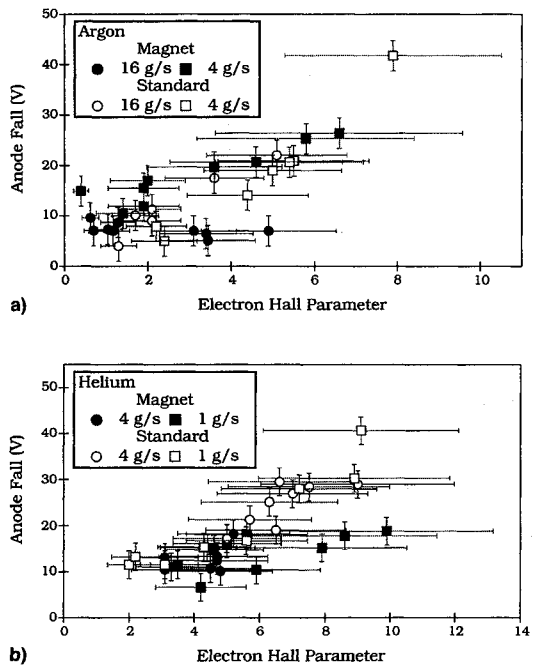

Fig. 14 Anode fall vs electron Hall parameter: a) argon and b) helium.

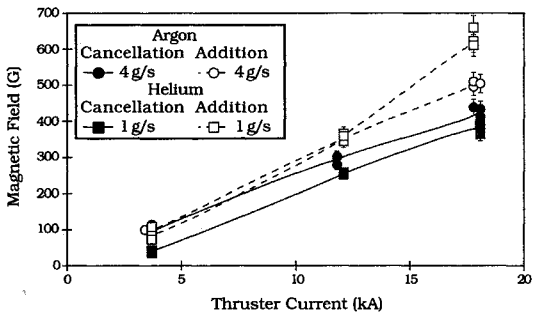

Fig. 15 Magnetic field measured downstream of anode lip.

stream of the anode midlip. Assuming that the electron temperature and ion number density remain constant along the lip, an assumption that is supported by previous studies,[8] the Hall parameter at the location of current attachment for these operating conditions will be significantly lower because of the lower magnetic field there. Thus, the MAHP anode operates at reduced anode falls (in comparison to the standard benchmark thruster) when the discharge current is forced to attach to the downstream portion of the anode by the magnetic field generated from the permanent magnets.

Figure 15 shows magnetic field strengths measured downstream of the anode midlip 3 mm away from the anode surface in both field enhancement and cancellation zones. This portion of the cancellation zones corresponds to where bands of peak luminosity are displayed in photographs of the discharge, which is assumed to be spots of current attachment. Unlike the data measured in the midlip, at high current the magnetic field strengths in the cancellation zones are significantly lower than those in the field addition zones. This trend is especially dramatic in the helium data at operating conditions in which the anode fall is most significantly reduced. Thus, the MAHP anode appears to have reduced the electron Hall parameter at locations of the anode where most of the current attaches.

Conclusions

The research presented in this article and others[9,25,26] has indicated that one method to reducing anode losses in MPD thrusters may be to decrease the electron Hall parameter in the vicinity of the anode. Since the electron Hall parameter is simply the ratio of the electron gyrofrequency to the electron collision frequency, anode designs which decrease the Hall parameter either by "decreasing the numerator (magnetic field)" or "increasing the denominator (collision frequency)" may be utilized to decrease anode losses.

In this study, an attempt was made at reducing the electron Hall parameter near the anode by decreasing the local magnetic field. By embedding permanent magnets within the anode of a benchmark thruster, thereby reducing the local Hall parameter in specific regions along the anode, a substantial decrease in anode losses was demonstrated at certain thruster operating conditions. Although crude, this experiment yielded promising results that clearly demonstrate the concept's potential for decreasing anode losses for a variety of current carrying devices.

Other electron Hall parameter reduction schemes may also be employed. Anode propellant injection may also serve as a means of decreasing anode losses. Proper coupling between the arc and the injected mass must be maintained to insure that the anode propellant does not decrease the performance of the thruster. However, if propellant is injected through an anode enclosure of relatively high pressure with a passage to pass current and propellant to the thrust chamber, the Hall parameter near the anode surface should be low by virtue of the large collision rates within the chamber.

Lastly, if the anode surface intersects the magnetic field lines allowing the electrons to simply "slide off" field lines onto the anode surface, a reduction of the anode fall should also follow. Studies conducted with an applied-field MPD thruster utilizing tandem electromagnet solenoids, wherein the angle of incidence of the axial magnetic field lines with respect to the anode surface were varied by adjusting the current levels of each solenoid, found that minimum anode heating rates were measured when the axial magnetic field lines that trapped the bulk of the discharge current intersected the anode surface (i.e., when current carrying electrons reached the anode surface without crossing field lines).[15] Thus, several approaches appear to have promise in reducing the anode power deposition.

Acknowledgments

This research was supported in part by NASA Contract 954997. The authors wish to thank George Miller for his technical assistance in the development of the MAHP anode.

References

[1]Garrison, P. W., Frisbee, R. H., and Pompa, M. F., "Ultra High Performance Propulsion for Planetary Spacecraft," FY'81 Final Rept., Jet Propulsion Lab. JPL D-2123, Jan. 1982.

[2]Babb, G. R., and Stump, W. R., "Comparison of Mission Design Options for Manned Mars Missions," *Manned Mars Missions, Working Group Papers*, edited by M. B. Duke and P. W. Keaton, NASA TM-89320, Vol. 1, Sec. 1-4, 1986, pp. 37–52.

[3]Palaszewski, B., "Electric Propulsion Parameters for Manned Mars Exploration," JANNAF Propulsion Meeting, Chemical Propulsion Information Agency, Laurel, MD, May 1989.

[4]Hack, K. J., George, J. A., Riehl, J. P., and Gilland, J. H., "Evolutionary Use of Nuclear Electric Propulsion," AIAA Paper 90-3821, Sept. 1990.

[5]Burton, R. L., Clark, K. E., and Jahn, R. G., "Measured Performance of a Multimegawatt MPD Thruster," *Journal of Spacecraft and Rockets*, Vol. 20, No. 3, 1983, pp. 229–304.

[6]Sovey, J. S., and Mantenieks, M. M., "Performance and Lifetime Assessment of Magnetoplasmadynamic Arc Thruster Technology," *Journal of Propulsion and Power*, Vol. 7, No. 1, 1991, pp. 71–83.

[7]Myers, R. M., "Applied-Field MPD Thruster Geometry Effects," AIAA Paper 91-2342, June 1991.

[8]Gallimore, A. D., Kelly, A. J., and Jahn, R. G., "Anode Power Deposition in Quasi-Steady MPD Thrusters," *Journal of Propulsion and Power*, Vol. 8, No. 6, 1992, pp. 1224–1231.

[9]Gallimore, A. D., Kelly, A. J., and Jahn, R. G., "Anode Power Deposition in MPD Thrusters," *Journal of Propulsion and Power*, Vol. 9, No. 3, 1993, pp. 361–368.

[10]Eckert, E. R. G., and Pfender, E., *Advances in Heat Transfer*, Vol. 2, edited by J. P. Harnet and T. F. Irvine Jr., Academic Press,

New York, 1967, pp. 229–316.
[11]Gallimore, A. D., "Anode Power Deposition in Coaxial MPD Thrusters," Ph.D. Dissertation, Dept. of Mechanical and Aerospace Engineering, Princeton Univ., Princeton, NJ, 1992.
[12]Subramaniam, V. V., and Lawless, J. L., "Electrode-Adjacent Boundary Layer Flow in Magnetoplasmadynamic Thrusters," *Physics of Fluids*, Vol. 31, No. 1, 1988, pp. 201–209.
[13]Randolph, T. M., personal communication, Princeton Univ., Princeton, NJ.
[14]Karkosak, J. J., and Hoffman, M. A., "Electrode Drops and Current Distribution in an MGD Channel," *AIAA Journal*, Vol. 3, No. 6, 1965, pp. 1198–1200.
[15]Schall, W., "Influence on Magnetic Fields on Anode Losses in MPD-Arcs," AIAA Paper 72-502, April 1972.
[16]Barnett, J. W., "Operation of the MPD Thruster with Stepped Current Input," Ph.D. Dissertation, Dept. of Mechanical and Aerospace Engineering, Princeton Univ., Princeton, NJ, 1985.
[17]Kurtz, H. L., Auweter-Kurtz, M., Merke, W. D., and Scharde, H. O., "Experimental MPD Thruster Investigations," AIAA Paper 87-1019, May 1987.
[18]Laframboise, J., "Theory of Cylindrical and Spherical Probes in a Collisionless Plasma at Rest," *Rarefied Gas Dynamics*, Vol. 2, edited by J. H. deLeeuw, Academic Press, New York, 1966, pp. 22–44.
[19]Peterson, E. W., and Talbot, L., "Collisionless Electrostatic Single-Probe Parameters by Means of Triple Probe," *AIAA Journal*, Vol. 8, No. 12, 1970, pp. 2215–2219.
[20]Tilley, D., "The Application of the Triple Probe Method to MPD Thruster Plumes," AIAA Paper 90-2667, July 1990.
[21]Tilley, D., Electric Propulsion Laboratory Progress Report 1776.23, Dept. of Mechanical and Aerospace Engineering, Princeton Univ., Princeton, NJ, Jan.–Feb. 1990.
[22]Hoskins, W. A., "Asymmetric Discharge Patterns in the MPD Thruster," M.S. Thesis, Dept. of Mechanical and Aerospace Engineering, Princeton Univ., Princeton, NJ, 1990.
[23]Jahn, R. G., *Physics of Electric Propulsion*, McGraw-Hill, New York, 1968, pp. 240–246.
[24]Choueiri, E. Y., Electric Propulsion Laboratory Progress Report 1776.14, Dept. of Mechanical and Aerospace Engineering, Princeton Univ., Princeton, NJ, March 1987.
[25]Choueiri, E. Y., "Electron-Ion Streaming Instabilities of an Electromagnetically Accelerated Plasma," Ph.D. Dissertation, Dept. of Mechanical and Aerospace Engineering, Princeton Univ., Princeton, NJ, 1991.
[26]Caldo, G., Choueiri, E. Y., Kelly A. J., and Jahn R. G., "An MPD Code with Anomalous Transport," AIAA Paper 91-102, Oct. 1991.